energies

MDPI

Article

Exergetic and Economic Evaluation of CO_2 Liquefaction Processes

Feng Chen and Tatiana Morosuk *

Institute for Energy Engineering, Technische Universität Berlin, 10587 Berlin, Germany; stefanchen0526@gmail.com
* Correspondence: tetyana.morozyuk@tu-berlin.de

Abstract: The transport of CO_2, as a part of the carbon capture and storage chain, has received increased attention in the last decade. This paper aims to evaluate the most promising CO_2 liquefaction processes that can be used for port-to-port and port–offshore CO_2 ship transportation. The energetic, exergetic, and economic analyses are applied. The liquefaction pressure has been set to 15 bar (liquefaction temperature −30 °C), which corresponds to the design of the existing CO_2 carriers. The three-stage vapor-compression process has been selected among closed systems (with propane-R290, ammonia-R717, and R134a as the working fluid) and the precooled Linde–Hampson process—as the open system (with R717). The three-stage vapor-compression process R290 shows the lowest energy consumption, and the CO_2 liquefaction cost 21.3 USD/tCO_2. Although the power consumption of precooled Linde–Hampson process is 3.1% higher than the vapor-compression process with R209, the lowest total capital expenditures are notable. The CO_2 liquefaction cost of precooled Linde–Hampson process is 21.13 USD/tCO_2. The exergetic efficiency of the three-stage vapor-compression process with R290 is 66.6%, while the precooled Linde–Hampson process is 64.8%.

Keywords: carbon dioxide; liquefaction; CO_2 ship transportation; exergy analysis; economic analysis

Citation: Chen, F.; Morosuk, T. Exergetic and Economic Evaluation of CO_2 Liquefaction Processes. *Energies* **2021**, *14*, 7174. https://doi.org/10.3390/en14217174

Academic Editor: Muhammad Abdul Qyyum

Received: 20 September 2021
Accepted: 19 October 2021
Published: 1 November 2021

1. Introduction

The CO_2 emission from the combustion of fossil fuels represented the most significant contributor to global warming, i.e., almost 80% of the total GWP [1]. Additionally, the upward trend of worldwide fossil fuels consumption as primary energy has not stopped [2]. The possibility that fossil fuels will remain dominant in power generation in the following years is high. Therefore, the feasible methods to mitigate the CO_2 emission from fossil fuel combustion have been suggested: improving the efficiency of the system [3]; implementing renewable energy sources [4]; and carbon capture and storage (CCS) [5].

The CCS chain consists of three main parts [6,7]: carbon capture, transportation, and storage or utilization. Figure 1 shows alternative options along the CCS chain. Many efforts have been made to develop efficient and economically effective carbon capture processes. Except for being stored, CO_2 can be utilized in industrial conversion processes [8]. The power-to-X options [9] give a new perspective for realizing the concepts of decarbonization in conjunction with demand response management and large implementation of renewable energy sources.

Geological CO_2 storage, which was proposed in the early 1990s, is the most technically feasible final step in the CCS chain. The two most ordinary geological storage methods are [9]:

- Saline aquifer storage. The CO_2 is injected into the saline aquifers without considering the potentially harmful effects for water sources (drinking water);
- Enhanced oil recovery. To reach the maximal economic oil recovery through the injection of CO_2 into the oil fields.

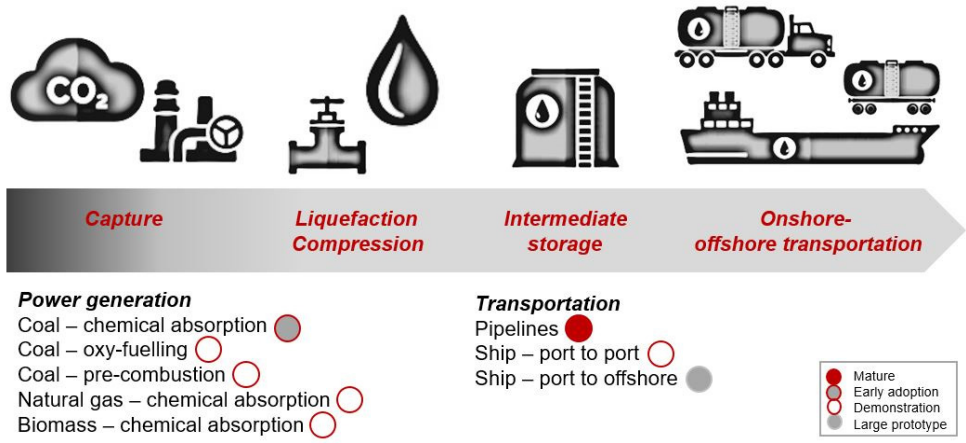

Figure 1. CCS chain. Alternative options and its Technology Readiness Level (adapted from [7]).

As the location of CO_2 storage is distributed, the transportation infrastructure should be developed to connect the capture and storage infrastructures. The available technologies are pipelines and ships (Figure 2). The pipelines are used under the circumstance of large-scale CO_2 and short transport distance. Purified CO_2 should be compressed above critical pressure (>73.8 bar) to ensure transportation in a single gas phase. For marine transport, the density of CO_2 is maximized through liquefaction. The pressure for marine transportation is slightly above the triple point (≥5.2 bar); however, CO_2 solidification should be avoided (due to spontaneous formation of dry ice in case of dropping the pressure during the loading/unloading). Therefore, for ship transportation, the recommended temperature and pressure of CO_2 are in the range between −30 and −50 °C that corresponds to 6 to 15 bar. CO_2 ship transportation is available on a small scale, making it economically non-competitive to pipeline transportation. At the same time, the advantage is that the initial investment is comparatively low, and it provides higher flexibility in terms of distance, client demand, and regulatory approval issues [7]. The large scale of marine transportation of CO_2 will have a potential in the future only under several conditions; one of them is the energetically efficient and economically feasible CO_2 liquefaction process. Recently, the International Energy Agency reported the market potential for CO_2-derived products and services [7]. The list of industrial participants includes Air Products and Chemical, Inc., Air Liquide, Linde AG, and other cryogenic companies. For example, "Full value chain CCS in one service" is offered by Aker Carbon Capture Company (Norway) [10].

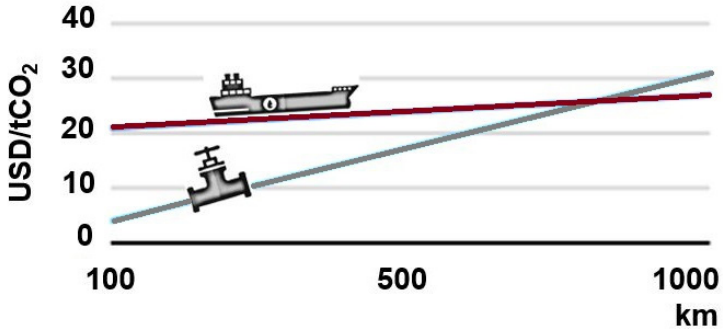

Figure 2. CO_2 transportation cost (adapted from [7]).

A very detailed study in the field of CCS chain is provided, for example, in [6,7,10]; however, the information about CO_2 liquefaction processes is not provided.

To demonstrate the scientific novelty of the authors' research, i.e., the feasibility study of the CO_2 liquefaction processes, the approach of the bibliometric analysis (using the Scopus database available in July 2021) was selected.

The bibliometric analysis started with the keyword "carbon dioxide" and resulted in 500+ thousand research publications since 1876. Only 12% of those publications were assigned to the energy field. The collection of the keywords that appeared in energy-related publications in the field of "carbon dioxide" during the time period 1921–2021 is shown in Figure 3a. The software VOSviewer was used for the identification of the links among the selected keywords [11].

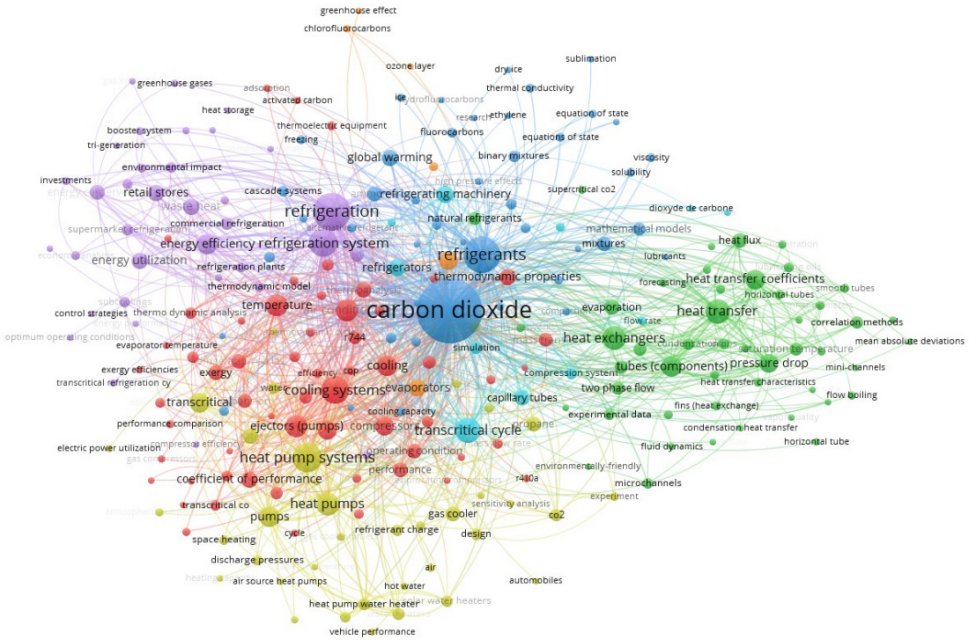

(**a**)

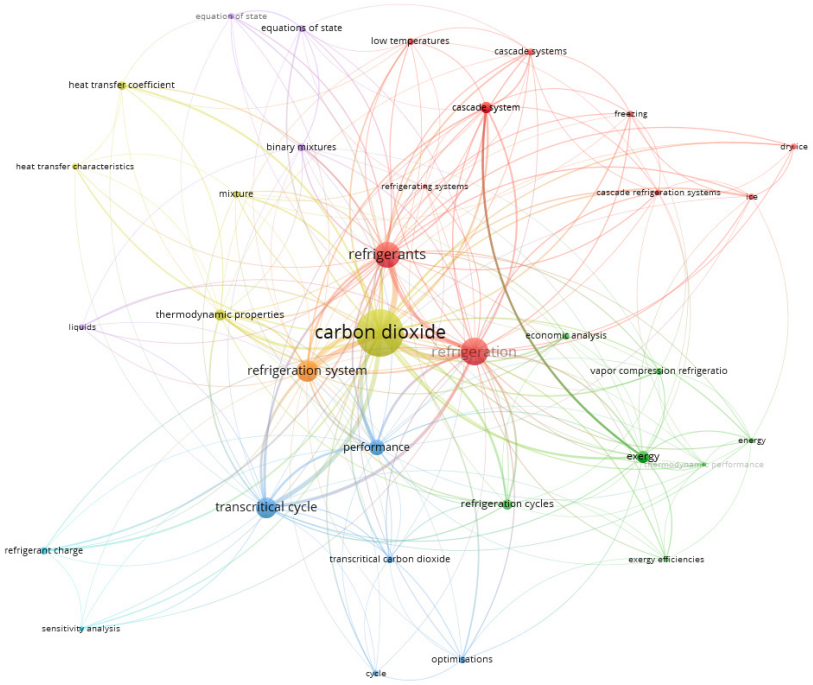

(**b**)

Figure 3. Co-occurrence and links among the keywords (by VOSviewer): (**a**) keyword "carbon dioxide", time period 1921–2021, and (**b**) filter "refrigeration", time period 2000–2021.

The research clusters are forming the areas of research: investigation of the properties of CO_2 (including mixtures), heat transfer characteristics and equipment, development in

the schematics, application of CO_2 as the working fluid for power and refrigeration systems, and the environmental impact of CO_2, etc. For example, the review and perspectives for the application of supercritical CO_2 thermodynamic cycles for power generation have been reported in the pioneering paper by Angelino [12]. The perspectives of CO_2 application for refrigeration systems as primary and secondary working fluid have been highlighted by Lorentzen [13]. R744 is the international nomenclature of CO_2 for refrigeration applications.

To describe the state-of-the-art in the field of authors' research, only publications limited by the keyword "refrigeration" (="cryogenics") were considered. As a result, 430 papers published over two decades formed the collection of the keywords shown in Figure 3b.

The review paper [14] perfectly described the progress in CO_2 refrigeration systems during the 20th century. However, the keyword "liquefaction" did not appear in this publication. This keyword did not form the cluster in Figure 1b (due to a relatively small number of publications).

The following papers, published during the last decade, demonstrate state-of-the-art in the field of large-scale CO_2 liquefaction for "port to port" or "port to offshore" transportation. The publications related to liquefaction CO_2 as a process within refrigeration systems and small-scale applications are not considered here.

Two types of CO_2 liquefaction processes were simulated with ASPEN HYSYS, and evaluated in [15]: conventional cascade refrigeration system (R744/R717) and single-refrigerant (R717) liquefaction cycle (similar to the nitrogen-based liquefied natural gas system). The reported thermodynamically optimal liquefaction pressure is 50 bar. The single-refrigerant cycle has 5% less power consumption. The irreversibilities were evaluated using Second Law efficiency; the value of 70% is reported for the single-refrigerant cycle. An economic analysis was not applied.

Effect of impurities (O_2, N_2, Ar, H_2, CO, H_2S, and CH_4) within CO_2 stream on operation conditions of liquefaction process, materials for equipment, storage system, and transportation is reported in [16]. Suitable pressure and temperature for CO_2 streams with very high purity are reported as 6 bar and −57 °C.

An extended study on impurities is reported in [17]. Different CCS technologies were evaluated where the liquefaction pressure varied between 7 and 70 bar. For pure CO_2, the specific cost of the liquefaction process is between 17.7 (7 bar) and 15.1 (70 bar) EUR/tCO_2. For amine-based post-combustion technology, the limit of CO_2 purity is reported as 99.94–99.86%, the specific cost of liquefaction process is 18.0 (7 bar)–15.4 (70 bar) EUR/tCO_2. The liquefaction of CO_2 (99.81–97.98%) after membrane-based post-combustion is calculated as 20.10 (7 bar)–15.5 (70 bar) EUR/tCO_2. Rectisol-based pre-combustion technology results in 99.33–98.42% purity and 18.90 (7 bar)–15.10 (70 bar) EUR/tCO_2. Regardless of CCS technology, the lower specific cost is associated with high pressure.

The CO_2 liquefaction under supercritical pressures 80–240 bar was evaluated in [18]. The electrical energy demand is directly proportional to the pressure and was found to be between 1.9 kWh/tCO_2 and 7.8 kWh/tCO_2.

The maximum CO_2 liquefaction pressure of 220 bar was fixed for the evaluation of four liquefaction cycles in [19]. The qualitative evaluation was applied to the following processes: gas compression of CO_2 (four-stage compression process) as base case; supercritical compression and pumping (four- and six-stage compression processes); subcritical compression and pumping (four- and six-stage compression processes), and so-called "refrigerated compression" (four-stage compression). The environmental temperature is assumed to be lower than critical. No quantitative data for liquefaction processes are available.

The evaluation of an entire CCS block has been performed in [20]; only relative values are reported. The CO_2 liquefaction system is based on a four-stage compression process. The goal was to achieve the maximum liquid yield. Economic analysis showed that the CO_2 liquefaction cost could be reduced from approximately 10.5 USD/tCO_2 to 9.9–10.0 USD/tCO_2. The condensation temperature is assumed to be equal to +10 °C (sea-

water is the cooling media). Such operation conditions make the cost of CO_2 liquefaction incomparable low.

Authors of [21] applied the cryogenic liquefaction cycles for CO_2 liquefaction. Four systems were evaluated: Linde–Hampson; Linde dual-pressure system; precooled Linde–Hampson system; and closed system. Sensitivity analysis was conducted to investigate the influence of parameters and selected systems on the life cycle cost. For the liquefaction pressure of 6 bar, the Linde–Hampson system and the Linde dual-pressure system are more economically effective, however the liquid yield is reduced.

A ship-based CCS chain with different CO_2 liquefaction pressures was evaluated economically in [22]. The goal of this research is to determine the optimal liquefaction pressure. Seven liquefaction pressures were suggested in order to cover the range between the triple point (5.18 bar/−56.6 °C) and the critical point (73.8 bar/31.1 °C). CCS chain was divided into five modules: a liquefaction system, storage tanks, a CO_2 carrier, storage tanks in the intermediate terminal, and a pumping system. The optimal liquefaction pressure is 15 bar (−27 °C).

For the first time, the boil-off CO_2 re-liquefaction processes were addressed in [23]. Pressures between 7 and 20 bar were considered (for different designs of the CO_2 ships). As only energy-related characteristics are relevant for ship application, the following results are reported: the CO_2 re-liquefaction fraction is between 0.524 (7 bar) and 0.997 (20 bar), and specific power consumption is between 187.8 kW/(tCO_2/h) for 7 bar and 260.0 kW/(t/hr) for 20 bar.

"Heat-pump-assisted CO_2 compression configurations" (the term used by authors) are examined in [24]. The CO_2 liquefaction pressure has been set to 57 bar. The performance is quantified in terms of net power consumption. The optimization using a genetic algorithm was applied and allowed for an 8% electric power saving and achieving 68% exergetic efficiency. In total, 44% of irreversibilities are associated with compressors, and 34% with intercooler and condenser (i.e., exergy transfer to the environment).

Four CO_2 liquefaction systems are compared in terms of energy, exergy, and economic performance in [25]. Exergoeconomic analysis was also performed. The authors proposed the integration of an absorption refrigeration system in order to increase the thermodynamic performance (exergetic efficiency is higher than 85%) and decrease the life cycle costs (for more than 20%). The conclusions are based on the exergoeconomic factors. The obtained results, unfortunately, cannot be used as references for this paper, as some initial data and assumptions for analysis are not available.

The reported findings have an overview of research on the CO_2 liquefaction processes. The exergy analysis was not applied often. The most promising CO_2 liquefaction processes reported in the above-mentioned publications were selected. This paper focuses on the evaluation of the ship-based CO_2 liquefaction systems with the help of exergy-based methods.

2. CO_2 Liquefaction Systems: Description and Modeling

Based on evaluated publications, the performance of the vapor-compression liquefaction process is the highest among all the closed liquefaction processes. Therefore, this process was selected as the closed system, and three working fluids were evaluated: R290, R7177, and R134a. For the open system, the precooled Linde–Hampson liquefaction process showed promising energetic and economic performance. Thus, the precooled Linde–Hampson liquefaction process with R717 as the working fluid was selected as an alternative to the open system.

The following assumptions were made for the simulation and evaluation of the CO_2 liquefaction systems:

- Large-scale CCS is assumed to be installed for a 500 MW pulverized coal-fired power plant, with results of 395 tCO_2/h.
- The CO_2 stream usually exits the CCS block under pressure 1.2–3.5 bar. The authors assumed the average value of 2 bar.

- Different kinds of CCS methods [17] provide the CO_2 stream with purity higher than 98%. For simplification, pure CO_2 is assumed to be liquefied.
- The optimal liquefaction pressure of the ship-based CO_2 liquefaction process has been reported as 15 bar. The authors assumed this value for simulation.
- The systems were simulated under steady-state conditions, assuming the adiabatic operation conditions for all components. The pressure drop in all heat exchanges is neglected.
- Heat exchanger for liquefaction process: minimal temperature difference is 3K.
- The outlet temperature for interstate coolers and condensers has been set to 30 °C.
- Compressors: maximum pressure ratio is 3, the isentropic efficiency is 0.85, and electrical efficiency is 0.95.

The flow diagram of the vapor-compression liquefaction process is shown in Figure 4. The captured CO_2 (stream 1) is compressed up to 15 bar (stream 5) by a two-stage compression process (CMP1 and CMP2) with interstate cooling and liquefied in the heat exchanger (HEAT). Stream 6 is liquid CO_2 under conditions for ship transportation. In the refrigerant cycle, stream 14–15 is used to remove the latent heat of the CO_2 during liquefaction. After, the three-stage compression process (stream 15–stream 7) with incomplete interstage cooling is used. Note, for R290 and R134a, only incomplete interstage cooling allows, while for R717 both, complete and incomplete are technically possible. For realizing the interstage cooling and achieving stream 14, three J-T valves in series (VAL1–VAL3) with two corresponding separators (SEP1 and SEP2) are implemented. Table 1 shows the simulation result of the three-stage vapor-compression CO_2 liquefaction process with different working fluids.

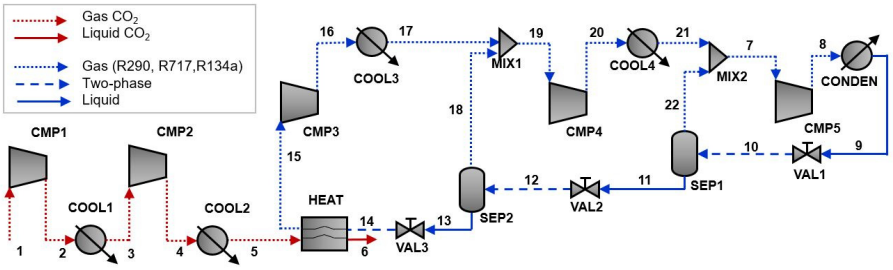

Figure 4. Three-stage vapor-compression CO_2 liquefaction process.

Table 1. The simulation result of three-stage vapor-compression CO_2 liquefaction process (Figure 4).

CO_2								
Parameters/States	**1**	**2**	**3**	**4**	**5**	**6**		
Temperature (°C)	30	115	30	116	30	−28		
Pressure (bar)	2.00	5.48	5.48	15.00	15.00	15.00		
Specific enthalpy (kJ/kg)	−8939	−8863	−8942	−886	−8951	−9311		
Specific exergy (kJ/kg)	37	104	92	157	145	208		
Mass flows rate (kg/s)	109.72	109.72	109.72	109.72	109.72	109.72		
R290								
Parameters/States	**7**	**8**	**9**	**10**	**11**	**12**	**13**	**14**
Temperature (°C)	26	54	30	6	6	−14	−14	−31
Pressure (bar)	5.74	10.81	10.81	5.74	5.74	3.05	3.05	1.62
Specific enthalpy (kJ/kg)	−2388	−2350	−2725	−2725	−2790	−2790	−2840	−2840
Specific exergy (kJ/kg)	91	124	110	106	110	107	113	111
Mass flows rate (kg/s)	123.08	123.08	123.08	123.08	101.60	101.60	88.69	88.69
Parameters/States	**15**	**16**	**17**	**18**	**19**	**20**	**21**	**22**
Temperature (°C)	15	41	30	−14	25	51	30	6
Pressure (bar)	1.62	3.05	3.05	3.05	3.05	5.74	5.74	5.74
Specific enthalpy (kJ/kg)	−2395	−2355	−2373	−2446	−2382	−2342	−2381	−2422
Specific exergy (kJ/kg)	25	60	59	62	59	94	97	92
Mass flows rate (kg/s)	88.69	88.69	88.69	12.91	101.60	101.60	101.60	21.47

Table 1. *Cont.*

R717								
Parameters/States	**7**	**8**	**9**	**10**	**11**	**12**	**13**	**14**
Temperature (°C)	28	98	30	6	6	−14	−14	−35
Pressure (bar)	5.31	11.58	11.58	5.31	5.31	2.44	2.44	0.94
Specific enthalpy (kJ/kg)	−2707	−2567	−3913	−3913	−4030	−4030	−4124	−4124
Mass flows rate (kg/s)	33.00	33.00	33.00	33.00	30.00	30.00	28.00	28.00
Parameters/States	**15**	**16**	**17**	**18**	**19**	**20**	**21**	**22**
Temperature (°C)	27	111	30	−14	27	96	30	6
Pressure (bar)	0.94	2.44	2.44	2.44	2.44	5.31	5.31	5.31
Specific enthalpy (kJ/kg)	−2695	−2514	−2693	−2785	−2699	−2555	−2702	−2754
Mass flows rate (kg/s)	27.61	27.61	27.61	2.07	29.68	29.68	29.68	3.01
R134a								
Parameters/States	**7**	**8**	**9**	**10**	**11**	**12**	**13**	**14**
Temperature (°C)	26	55	30	6	6	−14	−14	−31
Pressure (bar)	3.63	7.69	7.69	3.63	3.63	1.71	1.71	0.81
Specific enthalpy (kJ/kg)	−8784	−8764	−8964	−8964	−8998	−8998	−9024	−9024
Mass flows rate (kg/s)	234.02	234.02	234.02	234.02	193.59	193.59	169.07	169.07
Parameters/States	**15**	**16**	**17**	**18**	**19**	**20**	**21**	**22**
Temperature (°C)	12.27	38.40	30.00	−13.91	24.63	51.86	30.00	6.18
Pressure (bar)	0.81	1.71	1.71	1.71	1.71	3.63	3.63	3.63
Specific enthalpy (kJ/kg)	−8791	−8770	−8778	−8814	−8782	−8761	−8780	−8801
Mass flows rate (kg/s)	169.07	169.07	169.07	24.52	193.59	193.59	193.59	40.43

The flow diagram of the precooled Linde–Hampson liquefaction process is shown in Figure 5. The captured CO_2 (stream 1) goes through the two-stage compression process with interstage cooling. Stream 5 is mixed with return stream 13, and stream 6 is further compressed up to 25 bar (stream 7). After cooling and liquefaction (stream 9), CO_2 is then expanded in J-T valve down to the target pressure and separated. Stream 11 is the product stream. For the refrigerant cycle, ammonia (R717) is selected as the working fluid as suggested in [21]. The ammonia stream (stream 14) is compressed by the two-stage compression process in order to achieve the condensation pressure. Stream 18 is then expanded. Stream 19–14 (R717) together with "return" CO_2 stream 12–13 formed so-called "cold composite curve" within 3-flow heat exchanger (HEAT) in order to liquefy the stream of CO_2, i.e., "hot composite curve".

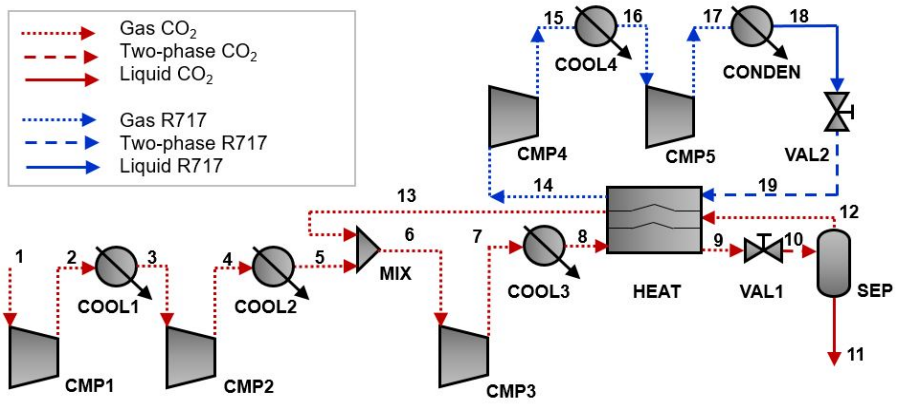

Figure 5. Precooled Linde–Hampson CO_2 liquefaction process.

3. Evaluation: Tools, Results, and Discussion

3.1. Energy Analysis

After simulation, the energy balances are applied to all systems' components. As a result, the total energy supply ($\dot{W}_{tot}$) and the required cooling duty for the simulated systems are given in Figure 6.

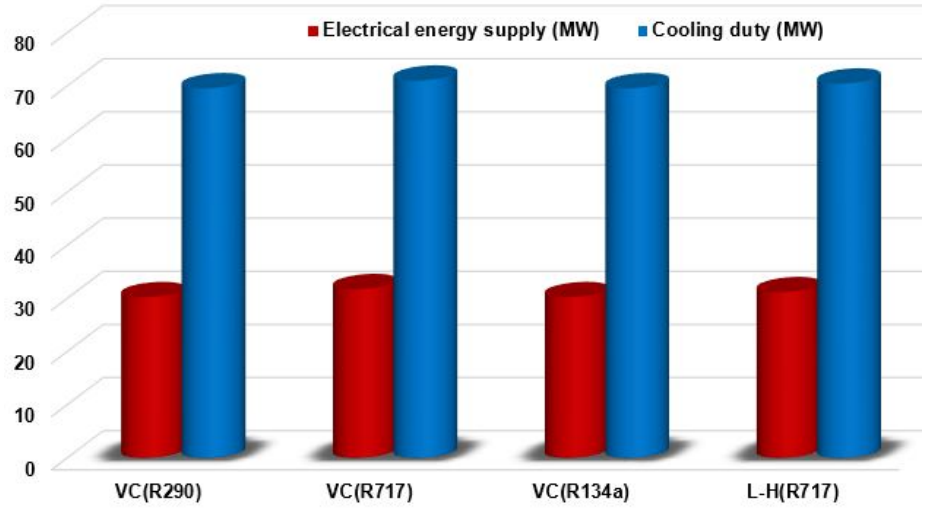

Figure 6. Comparison based on energy analysis.

The only variable that describes that energetic performance of the evaluated refrigeration system is the coefficient of performance (*COP*), as the inverse thermodynamic cycles are involved

$$COP = \frac{positive\ effect}{sup\ plied\ energy} = \frac{\dot{m}_{CO2}\left(h^{in}_{CO2} - h^{out}_{CO2}\right)}{\dot{W}_{tot}} \quad (1)$$

The *positive effect* is 40.82 MW. Therefore, the *COP* values are: 1.35 (VC R290), 1.29 (VC R717), 1.35 (VC R134a), and 1.31 (L-H R717).

The *COP* value cannot be applied for liquefaction as a "stand-alone" process (process 5–6 in Figure 4 and process 8–9 in Figure 5). The entire system for compression and liquefaction of the CO_2 stream must be considered. Note that the concept of *COP* of Carnot cycle is not meaningful to apply to the evaluated systems in order to make conclusions regarding the irreversibilities (including calculation of the second law efficiency).

The vapor-compression processes with R290 demonstrates the highest energetic performance, therefore has been further evaluated using the exergetic analysis. The vapor-compression process with R717 is less efficient; however, the same working fluid used for precooled Linde–Hampson process is comparable to VC R290 (Figure 6). The cooling duty required for any of the systems with R717 is slightly higher.

3.2. Exergetic Analysis

The exergetic analysis was applied to VC R290 and L-H R717 systems. The reference conditions have been set to 20 °C and 1.013 bar. The only physical exergy was calculated, and results are given in Tables 1 and 2 for corresponding systems. The exergy balances are written using the approach "exergy of fuel/exergy of product" [26].

Note that within the exergy balance for the overall system

$$\dot{E}_{F,tot} = \dot{E}_{P,tot} + \sum_{k} \dot{E}_{D,k} + \dot{E}_{L,tot} \quad (2)$$

the term $\dot{E}_{L,tot}$ is vanished, as all coolers and condenser within each evaluated system are assigned as dissipative components.

Table 2. The simulation result of the precooled Linde–Hampson CO_2 liquefaction process (Figure 5).

CO_2							
Parameters/States	**1**	**2**	**3**	**4**	**5**	**6**	**7**
Temperature (°C)	30	115	30	116	30	30	73
Pressure (bar)	2.00	5.48	5.48	15.00	15.00	15.00	25.00
Specific enthalpy (kJ/kg)	−8939	−8864	−8942	−8869	−8952	−8952	−8919
Specific exergy (kJ/kg)	37	104	92	157	145	145	174
Mass flows rate (kg/s)	109.72	109.72	109.72	109.72	109.72	124.52	124.52
Parameters/States	**8**	**9**	**10**	**11**	**12**	**13**	
Temperature (°C)	30	−12	−28	−28	−28	27	
Pressure (bar)	25.00	25.00	15.00	15.00	15.00	15.00	
Specific enthalpy (kJ/kg)	−8962	−9275	−9275	−9311	−9006	−8954	
Specific exergy (kJ/kg)	170	204	201	208	149	145	
Mass flows rate (kg/s)	124.52	124.52	124.52	109.72	14.80	14.80	
R717							
Parameters/States	**14**	**15**	**16**	**17**	**18**	**19**	
Temperature (°C)	19	88	30	102	30	−15	
Pressure (bar)	2.37	5.24	5.24	11.58	11.58	2.37	
Specific enthalpy (kJ/kg)	−2715	−2572	−2702	−2558	−3913	−3913	
Specific exergy (kJ/kg)	120	245	230	357	296	275	
Mass flows rate (kg/s)	31.84	31.84	31.84	31.84	31.84	31.84	

The exergetic efficiency of the overall system is

- vapor-compression

$$\varepsilon_{VC} = \frac{\dot{E}_{P,tot}}{\dot{E}_{F,tot}} = \frac{\left(\dot{E}_6 - \dot{E}_1\right)}{\dot{W}_{tot}} \tag{3}$$

- precooled Linde–Hampson

$$\varepsilon_{L-H} = \frac{\dot{E}_{P,tot}}{\dot{E}_{F,tot}} = \frac{\left(\dot{E}_{11} - \dot{E}_1\right)}{\dot{W}_{tot}} \tag{4}$$

Table 3 summarizes some results from the exergetic analysis. Figure 7 shows the distribution of the exergy destruction among the system components.

Table 3. The result of exergy analysis of the system.

	Fuel, $\dot{E}_{P,tot}$(MW)	**Product, $\dot{E}_{P,tot}$(MW)**	**Destruction, $\sum_k \dot{E}_{D,k}$ (MW)**	**Exergetic Efficiency, ε (%)**
VC (R290)	34.34	22.88	11.46	66.6
L-H (R717)	35.28	22.88	12.40	64.8

In the three-stage vapor-compression process, 41% of the total exergy destruction is associated with dissipative components (in yellow, Figure 7a), and 9% of the total exergy destruction with J-T valves and mixing units. For precooled Linde–Hampson process, 45% of the total exergy destruction is associated with dissipative components (in yellow, Figure 7b), and 8% of the total exergy destruction with J-T valves.

The obtained results are comparable to the ones reported in [24]. The options for thermodynamic improvement of both systems should definitely include an increase in the isentropic efficiency of compressors. The application of the advanced exergy analysis [27] will not bring benefit for the evaluation of the system due to the large number of (a) dissipative components, and (b) components with a high percentage of the unavoidable exergy destruction (J-T valves and mixing units).

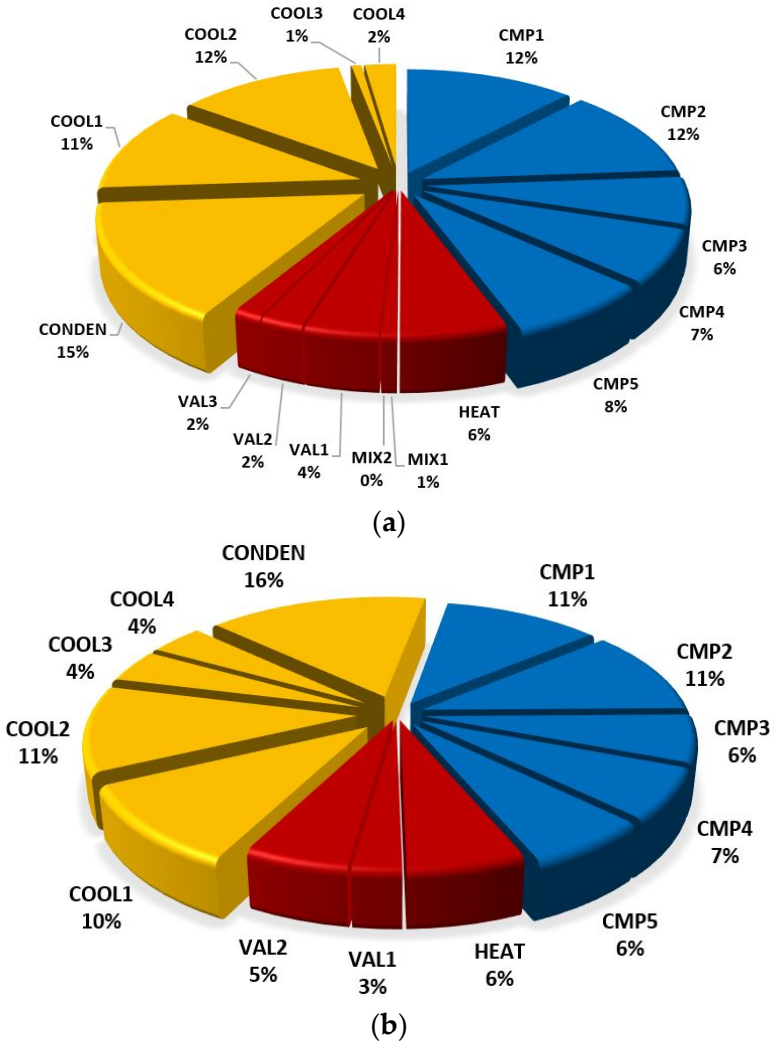

Figure 7. Exergy destruction of components: (**a**) vapor-compression process with R 290; (**b**) precooled Linde–Hampson process with R717.

3.3. Economic Analysis

As the simulation was performed in Aspen Plus, the most convenient method is to ascertain the equipment cost data directly from Aspen Process Economic Analyzer® in US dollars for January 2019. The obtained data were adjusted to March 2021 using cost indices.

The assumptions used for the economic analysis:

- Project life—25 years;
- Construction time—2 years;
- Interest rate—7.5%;
- Operating hours per year—8000;
- Electricity cost—0.173 USD/kWh;
- Cooling water cost—0.029 USD/kWh.

The relative results obtained from the economic analysis are given in Figure 8. To report the absolute numbers is not meaningful, as these numbers are linked to the capacity of CCS block within a power plant and the corresponding CO_2 liquefaction system. However, the specific cost of the entire liquefaction process is essential (Figure 9). The conclusions obtained from economic analysis do not contradict the energetic analysis: the most effective systems are VC R290 (21.30 USD/tCO_2) and L-H R717 (21.13 USD/tCO_2).

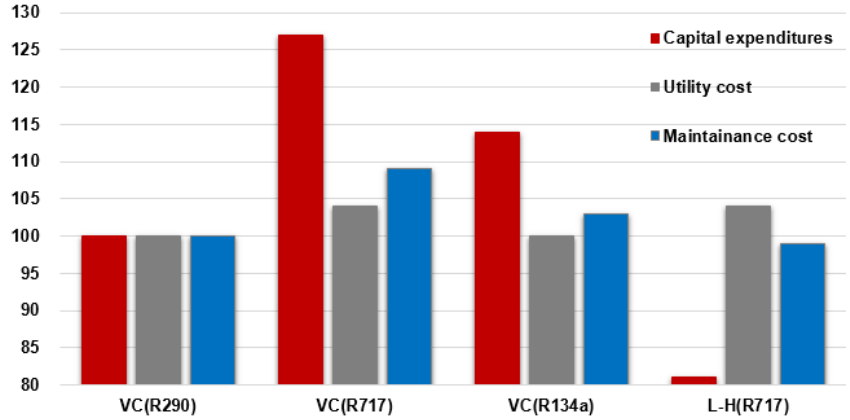

Figure 8. Relative results obtained from the economic analysis (VC R290 is assumed to be a reference case, 100%).

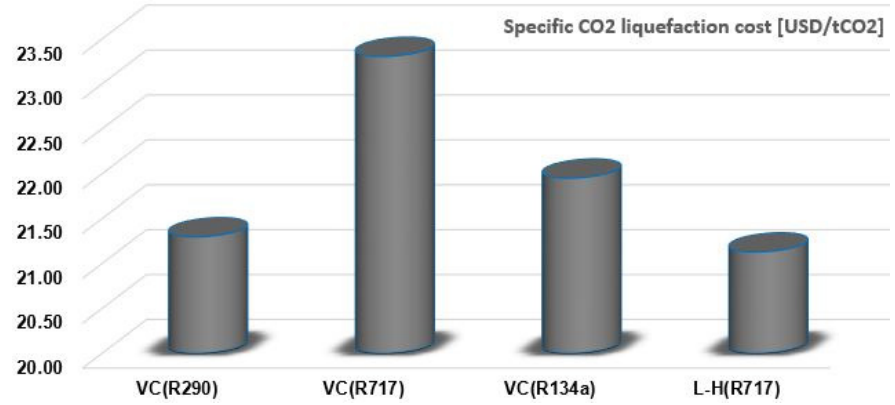

Figure 9. Specific CO_2 liquefaction cost (March 2021).

The exergoeconomic analysis [26] was not applied to the evaluated systems. Based on the authors' experience [28], the cost of exergy destruction will dominate within the majority of components. The only structure-parametric optimization should be used in order to improve both, VC and L-H, systems.

4. Conclusions

This paper reports the results of an exergetic and economic investigation of three vapor-compression (closed system) and one precooled Linde–Hampson processes. All systems are evaluated for potential use for the ship-based CO_2 liquefaction processes. The liquefaction pressure of CO_2 has been set to 15 bar to fit the design of the available CO_2 carriers.

After determining the most energy-efficient and economically feasible working fluid for the three-stage vapor-compression process, i.e., R290, the exergetic analysis was performed. Additionally, the exergetic analysis was applied to precooled Linde–Hampson process (only R717 as the working fluid was considered).

The vapor-compression process with R290 has finally been testified to have the best energetic and economic performance. The power consumption of precooled Linde–Hampson process is 3.1% higher, and the cost of the liquefaction process is higher as well.

The obtained results cannot be directly compared to the results reported by others due to different (a) boundary conditions, (b) approaches for conducting the exergetic analysis, and (c) scaling for economic analysis.

Multi-objective optimization is the next research step.

Author Contributions: Conceptualization, F.C. and T.M.; methodology, T.M.; software, F.C.; validation, F.C.; formal analysis, F.C.; investigation, F.C. and T.M.; resources, F.C. and T.M.; data curation, F.C. and T.M.; writing—original draft preparation, F.C.; writing—review and editing, T.M.; visualization, F.C. and T.M.; supervision, T.M. All authors have read and agreed to the published version of the manuscript.

Funding: This research received no external funding.

Conflicts of Interest: The authors declare no conflict of Interest.

References

1. Environmental Protection Agency. Inventory of U.S. Greenhouse Gas Emissions and Sinks. Available online: https://www.epa.gov/ghgemissions/inventory-us-greenhouse-gas-emissions-and-sinks (accessed on 20 September 2021).
2. Energy Information Adminstration. U.S. Energy Facts Explained. Available online: https://www.eia.gov/energyexplained/us-energy-facts/ (accessed on 20 September 2021).
3. Xu, C.; Xu, G.; Zhao, S.; Dong, W.; Zhou, L.; Yang, Y. A Theoretical Investigation of Energy Efficiency Improvement by Coal Pre-Drying in Coal Fired Power Plants. *Energy Convers. Manag.* **2016**, *122*, 580–588. [CrossRef]
4. Schnitzer, H.; Brunner, C.; Gwehenberger, G. Minimizing Greenhouse Gas Emissions through the Application of Solar Thermal Energy in Industrial Processes. *J. Clean. Prod.* **2007**, *15*, 1271–1286. [CrossRef]
5. Bui, M.; Adjiman, C.S.; Bardow, A.; Anthony, E.J.; Boston, A.; Brown, S.; Fennell, P.S.; Fuss, S.; Galindo, A.; Hackett, L.A.; et al. Carbon Capture and Storage (CCS): The Way Forward. *Energy Environ. Sci.* **2018**, *11*, 1062–1176. [CrossRef]
6. Noh, H.; Kang, K.; Huh, C.; Kang, S.-G.; Han, S.J.; Kim, H. Conceptualization of CO_2 Terminal for Offshore CCS Using System Engineering Process. *Energies* **2019**, *12*, 4350. [CrossRef]
7. International Energy Agency. Energy Technology Perspectives 2020 Foreword Special Report on Carbon Capture, Utilisation and Storage. Available online: https://iea.blob.core.windows.net/assets/181b48b4-323f-454d-96fb-0bb1889d96a9/CCUS_in_clean_energy_transitions.pdf (accessed on 20 September 2021).
8. Alper, E.; Orhan, O.Y. CO_2 utilization: Developments in conversion processes. *Petroleum* **2017**, *3*, 109–126. [CrossRef]
9. Koj, J.C.; Wulf, C.; Zapp, P. Environmental impacts of power-to-X systems—A review of technological and methodological choices in Life Cycle Assessments. *Renew. Sustain. Energy Rev.* **2019**, *112*, 865–879. [CrossRef]
10. Aker Carbon Capture Company, Norway. 2020. Available online: https://akercarboncapture.com/offerings/carbon-capture-as-a-service/ (accessed on 20 September 2021).
11. Van Eck, N.; Waltman, L. Software survey: VOSviewer, a computer program for bibliometric mapping. *Scientometrics* **2010**, *84*, 523–538. [CrossRef]
12. Angelino, G. Carbon Dioxide Condensation Cycles for Power Production. *J. Eng. Power ASME* **1968**, *90*, 287–295. [CrossRef]
13. Lorentzen, G. Revival of carbon dioxide as a refrigerant. *Int. J. Refrig.* **1994**, *17*, 292–300. [CrossRef]
14. Kim, M.-H.; Pettersen, J.; Bullard, C.W. Fundamental process and system design issues in CO_2 vapor compression systems. *Prog. Energy Combust. Sci.* **2004**, *30*, 119–174. [CrossRef]
15. Alabdulkarem, A.; Hwang, Y.; Radermacher, R. Development of CO_2 Liquefaction Cycles for CO_2 Sequestration. *Appl. Therm. Eng.* **2012**, *33–34*, 144–156. [CrossRef]
16. Wetenhall, B.; Aghajani, H.; Chalmers, H.; Benson, S.D.; Ferrari, M.-C.; Li, J.; Race, J.M.; Singh, P.; Davison, J. Impact of CO_2 impurity on CO_2 compression, liquefaction and transportation. *Energy Procedia* **2014**, *63*, 2764–2778. [CrossRef]
17. Deng, H.; Roussanaly, S.; Skaugen, G. Techno-economic analyses of CO_2 liquefaction: Impact of product pressure and impurities. *Int. J. Refrig.* **2019**, *103*, 301–315. [CrossRef]
18. Engel, F.; Kather, A. Improvements on the Liquefaction of a Pipeline CO_2 Stream for Ship Transport. *Int. J. Greenh. Gas Control* **2018**, *72*, 214–221. [CrossRef]
19. Yoo, B.Y.; Lee, S.G.; Rhee, K.P.; Na, H.S.; Park, J.M. New CCS System Integration with CO_2 Carrier and Liquefaction Process. *Energy Procedia* **2011**, *4*, 2308–2314. [CrossRef]
20. Lee, U.; Yang, S.; Jeong, Y.S.; Lim, Y.; Lee, C.S.; Han, C. Carbon Dioxide Liquefaction Process for Ship Transportation. *Ind. Eng. Chem. Res.* **2012**, *51*, 15122–15131. [CrossRef]
21. Seo, Y.; You, H.; Lee, S.; Huh, C.; Chang, D. Evaluation of CO_2 Liquefaction Processes for Ship-Based Carbon Capture and Storage (CCS) in Terms of Life Cycle Cost (LCC) Considering Availability. *Int. J. Greenh. Gas Control* **2015**, *35*, 1–12. [CrossRef]
22. Seo, Y.; Huh, C.; Lee, S.; Chang, D. Comparison of CO_2 Liquefaction Pressures for Ship-Based Carbon Capture and Storage (CCS) Chain. *Int. J. Greenh. Gas Control* **2016**, *52*, 1–12. [CrossRef]
23. Lee, Y.; Baek, K.H.; Lee, S.; Cha, K.; Han, C. Design of boil-off CO_2 re-liquefaction processes for a large-scale liquid CO_2 transport ship. *Int. J. Greenh. Gas Control* **2017**, *67*, 93–102. [CrossRef]
24. Muhammada, H.A.; Roha, C.; Choa, J.; Rehmanc, Z.; Sultanb, H.; Baika, Y.-J.; Lee, B. A comprehensive thermodynamic performance assessment of CO_2 liquefaction and pressurization system using a heat pump for carbon capture and storage (CCS) process. *Energy Convers. Manag.* **2020**, *206*, 112489. [CrossRef]
25. Aliyon, K.; Mehrpooya, M.; Hajinezhad, A. Comparison of Different CO_2 Liquefaction Processes and Exergoeconomic Evaluation of Integrated CO_2 Liquefaction and Absorption Refrigeration System. *Energy Convers. Manag.* **2020**, *211*. [CrossRef]

26. Bejan, A.; Tsatsaronis, G.; Moran, M. *Thermal Design and Optimization*; John Wiley and Sons: New York, NY, USA, 1996.
27. Morosuk, T.; Tsatsaronis, G. Advanced Exergetic Evaluation of Refrigeration Machines Using Different Working Fluids. *Energy* **2009**, *34*, 2248–2258. [CrossRef]
28. Fazelpour, F.; Morosuk, T. Exergoeconomic analysis of carbon dioxide transcritical refrigeration machines. *Int. J. Refrig.* **2014**, *38*, 128–139. [CrossRef]